Theoretical Consideration Regarding Static Loading of the Right Ventricle During Resuscitation

Resüssitasyon Boyunca Sağ Ventrikülün Statik Yüklenmesine Dair Teorik Düşünce

ORCID IDs of the authors: L.C. 0000-0003-3331-6557; J.S. 0000-0002-7566-4632; C.G. 0000-0001-6582-6055.

Dear Editor,

Is it possible that rapid volume infusion during resuscitation efforts may directly cause right heart failure? Many clinicians believe so. The Belmont® Rapid Infuser (Belmont Instrument Corporation, Billerica, MA) can infuse fluids at a rate of up to 750 mL min^{-1} and is often run continuously for extended periods of time. This rapid increase in volume and, therefore, venous return, could potentially cause acute right heart failure if the heart is unable to accommodate this additional volume in trauma resuscitation efforts.

Ventricular preload, or filling, affects the stretch of the myocardial sarcomeres. The sarcomeres behave according to the Frank–Starling mechanism (1). In the cardiac muscle, the length–tension curve is steeper than in the skeletal muscle, and it is shifted towards the right, denoting the need for increased cardiac sarcomere length in comparison to skeletal muscle to achieve the same tension (Figure 1) (1).

The right ventricle (RV) is considered to be more sensitive to changes in pressure than it is to changes in volume (2). The question arises whether it is possible to infuse fluids to a continuously euvolemic patient (i.e. volume administered equals the volume lost from haemorrhage) so rapidly that the right heart fails. Because the right heart is better able to accommodate acutely increased preload, we hypothesise that additional volume from rapid fluid infusion will cause heart enlargement, but not to a degree that would cause right heart failure.

To mathematically test this hypothesis, the RV was modelled as an ellipsoid to determine 1) how much fluid infusion stretches the sarcomeres and 2) whether this stretch theoretically causes the sarcomeres to exceed their peak tension on the Frank–Starling curve. Figure 2 shows an ellipsoid shell subtraction model developed by Feneley et al. (3), to better approximate the shape of the RV. The ellipsoid model mimics the crescent-shaped anatomy of the heart. The right ventricular dimensions provided by data from "Guidelines for the Echocar-

diographic Assessment of the Right Heart in Adults," (4) were used for further calculations. In this paper, the RV septal-to-free wall diameter average is 2.8 cm, and the RV average height is 7.1 cm. According Feigenbaum's Echocardiography, the left ventricular diastolic diameter average is 5.05 cm (5). Assuming that the RV is two-thirds the height of the left ventricle (LV), this gives an average LV height of 11.25 cm. The calculations for the ellipsoid subtraction model are shown in Appendix 1.

The equation for the right ventricular volume developed by Feneley et al. is RVV= $\left(\frac{\pi}{6}\right)$ (abd)–FWV, with 'a' being the RV height, 'b' being the LV diastolic diameter, 'd' being the RV septal-to-free wall diameter, and FWV being the free wall volume (3). The free wall volume is assumed to be constant for subsequent calculations. Therefore, the free wall volume can be removed from the equation when calculating the change in the volume. To adjust the dimensions to see how they would change with varying end diastolic volumes (EDVs), the dimensions were converted into proportions based on one diameter, 'd'. Once this was calculated, the equation was arranged in terms of the volume, V= $\frac{d^3}{0.194}$, and the new RV septal-to-free wall diameter ('d') was determined.
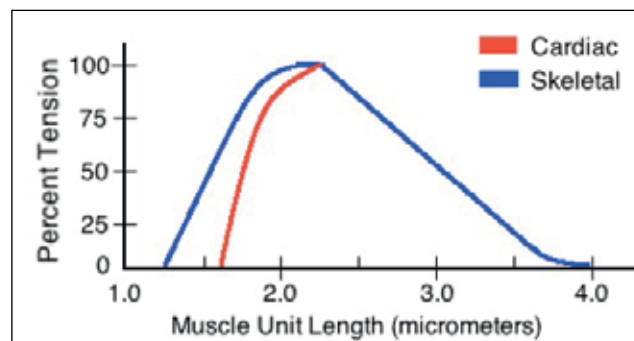

Figure 1. Schematic of the muscle unit length-tension relationship for the cardiac muscle (red) and skeletal muscle. Modified from Shiels et al. (1)
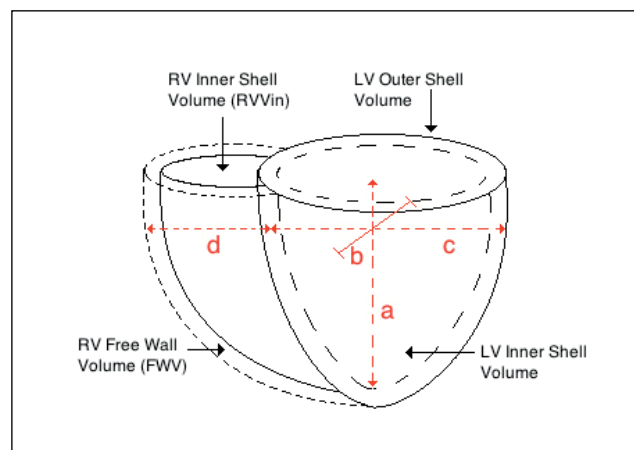

Figure 2. Diagram of the ellipsoid shell subtraction model showing the different dimensions used in the calculations for percent stretch. Modified from Feneley et al. (3)

For the calculations of the percent stretch after infusion, it was only necessary to look at one dimension (RV septal-to-free wall diameter) because the model was built to proportionately increase in all directions as volume increases. Since the radius is directly proportional to the circumference, the radius can replace the circumference in calculating the percent stretch. Because the difference between the RV radius and the RV septal-to-free wall diameter is a constant ratio, the RV septal-to-free wall diameter can be used to compare its initial length to determine the percent stretch. The infusion rate needed to bring the EDV to the peak EDV of the Frank-Starling curve was also calculated, as mentioned above.

The following parameters were varied in the model: infusion rate, heart rate (HR) and cardiac output (CO). Infusion rates of 500, 750, 1000 and 1500 mL min^{-1} were chosen because, clinically, the Belmont® Rapid Infuser can infuse fluids at a rate of up to 750 mL min^{-1}. HRs of 60, 90 and 120 beats min^{-1} were used in this model to illustrate a range of physiologic
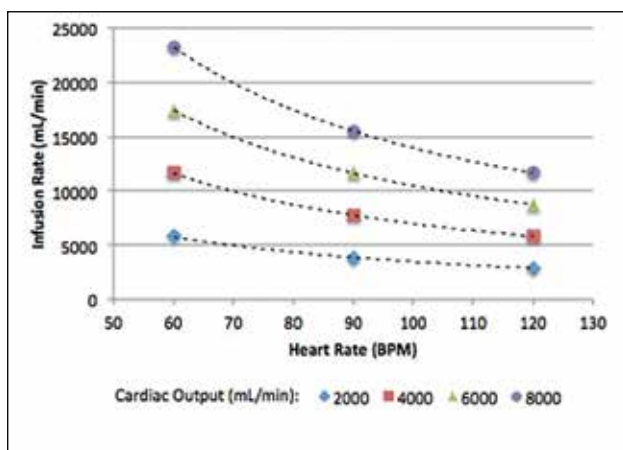

Figure 3. Ellipsoid model end diastolic volume at the peak of the Frank-Starling curve for the sarcomeres (40% stretch) at different heart rates and cardiac outputs
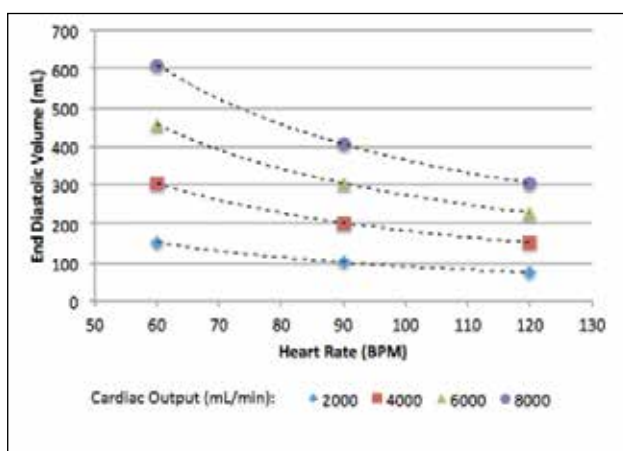

Figure 4. Ellipsoid model infusion rate needed to increase the end diastolic volume to the peak of the Frank-Starling curve for the sarcomeres (40% stretch) at different heart rates and cardiac outputs

states. Patients often arrive to the operating room tachycardic from haemorrhage or anxiety. Conversely, some are bradycardic from prior beta-blockade medication. The pre-infusion CO values used were 2, 4, 6 and 8 L min^{-1} because this range encompasses multiple physiologic resuscitation scenarios. Combinations of different infusion rates, HRs and COs were used to observe how changing each of these variables would affect the amount of stretch in the RV model.

Resting cardiac sarcomere length is approximately 1.6 μm (1). The peak tensile strength of cardiac sarcomeres is reached when the sarcomere is stretched to around 2.25 μm (1). Dividing L_{max} (2.25 μm) by the resting sarcomere length (1.6 μm) yields a 40% stretch between resting and optimal length, which was used as the limit at which the RV would be overloaded. The stretch of the ellipsoid model of the RV was determined based on different combinations of varying HR, CO and, by extension, EDV, as well as the superimposed infusion rate.

As seen in Table 1, at a constant HR, the EDV increases with increasing CO. At a constant CO, the EDV decreases with increasing HR. Varying all these parameters, the percent stretch from baseline EDV never exceeded 13.2%. This amount of stretch (13.2%) was reached at a CO of 2000 mL min^{-1} and an infusion rate of 1500 mL min^{-1}, irrespective of HR (see Appendix 2). The minimum incremental stretch was 1.2% at a CO of 8000 mL min^{-1} and an infusion rate of 500 mL min^{-1}. The percent stretch after infusion of 500 mL min^{-1} and 1000 mL min^{-1} is shown in Tables 1 and 2, respectively. For percent stretch at other infusion rates, see Appendix 2.

The EDV and infusion rates that will result in a 40% stretch of the RV are plotted in Figure 3 (EDV) and Figure 4 (infusion rates) for the three HRs and COs. The line of best fit was included for each of the COs. For each line of best fit, the correlation coefficient (r^2) was 1, which shows the strength of the relationship between the variables. For example, as shown in Figure 3, at an HR of 90 beats min^{-1} and a CO of 4 L min^{-1}, the EDV would need to be approximately 200 mL for the RV to be stretched 40% from baseline, which had an initial EDV of 74 mL. To achieve this, an infusion rate of approximately 7.7 L min^{-1} would be needed (Figure 4). Each combination of different parameters (HR, infusion rate, CO) results in a different baseline EDV and therefore a different EDV for a 40% stretch. The EDV with a 40% stretch ranged from 76.2 to 609.8 mL.

In this ellipsoid subtraction model of the RV, all of the clinical variables used for COs, HRs and infusion rates, failed to surpass the 40% stretch of sarcomeres. Furthermore, the maximum stretch calculated was found to be 13.2% that occurred with an infusion rate of 1500 mL min^{-1} and a CO of 2 L min^{-1}. Additionally, the range of infusion rates that would cause a 40% stretch in the ellipsoid model using the various COs was calculated and found to be 2.9 to 23.2 L min^{-1}.

Furthermore, the lower limit infusion rate of 2.9 L min^{-1} is well above the infusion rate that the Haemonetics® Rapid Infusion System provides. These mathematical models of the RV suggest that massive amounts of fluid in isolation would be required to overcome the RV's ability to tolerate the excess preload in a euvolemic patient. This amount of fluid is greater than what can be infused by typical rapid infusion systems like the Belmont® Rapid Infuser and the Haemonetics® Rapid Infusion System.

Table 1. Percent Stretch from Baseline with an Infusion Rate of 500 mL min^{-1} at Varying Heart Rates and Cardiac Outputs

HR (bpm)	CO (mL min^{-1})	EDV (mL)	EDV during Infusion (mL)	% Stretch
60	2000	55.6	63.9	4.8
60	4000	111.1	119.4	2.4
60	6000	166.7	175.0	1.6
60	8000	222.2	230.5	1.2
90	2000	37.0	42.6	4.8
90	4000	74.1	79.7	2.4
90	6000	111.1	116.7	1.6
90	8000	148.1	153.7	1.2
120	2000	27.8	31.9	4.8
120	4000	55.6	59.8	2.4
120	6000	83.3	87.5	1.6
120	8000	111.1	115.3	1.2

HR: heart rate; CO: cardiac output; EDV: end diastolic volume

Table 2. Percent Stretch from Baseline with an Infusion Rate of 1000 mL min^{-1} at Varying Heart Rates and Cardiac Outputs

HR (bpm)	CO (mL min^{-1})	EDV (mL)	EDV During Infusion (mL)	% Stretchh
60	2000	55.6	72.2	9.1
60	4000	111.1	127.8	4.8
60	6000	166.7	183.3	3.2
60	8000	222.2	238.9	2.4
90	2000	37.0	48.1	9.1
90	4000	74.1	85.2	4.8
90	6000	111.1	122.2	3.2
90	8000	148.1	159.2	2.4
120	2000	27.8	36.1	9.1
120	4000	55.6	63.9	4.8
120	6000	83.3	91.7	3.2
120	8000	111.1	119.4	2.4

HR: heart rate; CO: cardiac output; EDV: end diastolic volume

Although these models suggest that the amount of fluid infused is not enough to cause RV failure if euvolemia is maintained, our assumptions and limitations do not allow us to conclude that rapid fluid infusions are safe in all clinical settings. We assumed baseline euvolemia for calculating the resting sarcomere length and that the volume infused did not accumulate in the RV. We also assumed that there was no change in the capacitance of the vessels throughout the body and that the pleural pressure remained constant. As the RV stretched with fluid infusion, we assumed that the sarcomeres stretched equally and that there was a uniform orientation of the myofilaments. The assumption that the mycotes are all oriented horizontally across the direction of tension will maximise the amount of stretch seen by the myocytes along the x-axis. For a myocyte oriented at different angles as opposed to those lying parallel, the myocyte may shrink slightly less to achieve the same amount of circumferential stretch along the x-axis. Although the limits for the length–tension curve for the sarcomeres are approximately 1.6 and 2.25 μm, these lengths may not be uniformly distributed because the lengths can slightly vary (6). There was also an assumption that there was no change in myocardial wall thickness or contractility and that the stretch and not strain was the cause of failure. Stress rather than strain determines muscular overload, and that determinant is largely affected by intracavitary pressures, ventricular wall thickness, and geometry of the wall (Laplace's law).

There are several limitations to these models. First, the RV is considered to be more sensitive to changes in pressure than it is to changes in volume (2). Thus, a similar model using these haemodynamic parameters should be made considering what effect this would have on the RV pressure. Consequently, the ventricular interdependence seen physiologically, where the LV's function would be influenced by an increase in the RV volume, is not demonstrated in these models. In states of the RV pressure overload, which can be seen during an RV volume overload, the LV filling is subsequently impaired. The dominant mechanism of this impairment is through series interaction, where the left atrium and LV filling are decreased because of a decreased RV output ensuing from an increased RV afterload (7). Direct interaction also takes place where the RV enlargement compresses the LV and impairs its filling (8). The impact of this fluid overload on the RV is mostly through its effects on the LV filling than the RV function itself. A severely compressed LV can result in pulmonary oedema, pulmonary hypertension and hypoxaemia. The increased RV afterload causes increased RA pressure.

These models also do not account for the compensatory mechanisms of the body with an increased preload. The RV, absent a negative inotropic influence, is able to accommodate large increases in preload without affecting functionality until it is distended past a certain point. This point is unknown. It is likely that the failure of the RV during distension is not

only accounted for by percent stretch, but also by wall tension, which is also determined by the wall thickness and HR (Treppe phenomenon). Our models use several combinations of HRs and COs to determine how these affect the EDV and stretch of the RV. Subsequently, these models do not account for the dynamic and compensatory nature of the body to the increased volume, ongoing losses and adaptive changes in peripheral resistance, which would affect pulmonary artery pressure and venous return.

The results of our models suggest that the volume effect of the fluid infusion by itself is unlikely the cause of heart failure occasionally seen on an echocardiogram initially during massive resuscitations. There are several other possibilities that could account for the decreased right heart function in these situations, one such cause being myocardial infarction from the physiologic stress of the resuscitation or from a myocardial oxygen supply/demand imbalance. Cardiac arrests can also precipitate from hyperkalaemic arrhythmias that may develop after massive amounts of banked blood products are transfused, which can be further exacerbated by the hypocalcaemic, hyperglycaemic, hypothermic and acidotic states that banked products may also create (9). A pulmonary embolism or some other cause of pulmonary hypertension may also cause heart failure in trauma patients undergoing fluid resuscitation due to a sudden increase in right-sided heart pressures. This can also cause ischaemia of the RV resulting from increased wall tension and oxygen demand, as well as decreased coronary perfusion from an under-filled LV (10). In addition to affecting coagulation, hypothermia also exerts a negative effect on heart contractility (11). At higher HRs, the maximum contraction may not be reached, further decreasing CO (11).

Calcium levels also affect cardiac contractility from calcium's role in excitation–contraction coupling. Heart failure resulting from hypocalcaemia has been described in patients with undiagnosed hypoparathyroidism presenting to the Emergency Department, even in the absence of underlying heart disease (12). For example, one patient with hypoparathyroidism was found to have a hypocalcaemic-induced cardiomyopathy resulting from an ionised calcium level of 0.75 mmol L^{-1} (nl 1.16–1.32 mmol L^{-1}) (12). In trauma resuscitation, it is possible that acute hypocalcaemia from citrated blood products could result in heart failure. In one study, at 5 minutes at the maximum infusion rate (150 mL min^{-1} in a 70 kg person) of citrated whole blood, the ionised calcium level decreased by 41% to approximately 0.65 mmol L^{-1} (13).

Another factor affecting ventricular filling and CO is the pericardium. The pericardium's stiffness exerts a greater effect on the filling pressures during fluid infusion on the right side of the heart than on the left (14). The effect of the pericardium would act to limit the amount of fluid delivered to the heart during large-volume infusion, which would result in decreased CO or a failure of CO increase when expected. The effects of the pericardium can be seen in the study by Hoit et al. that looked at the effects of a pericardiectomy on the right and left ventricular filling and showed that the filling of the ventricles is restricted by the pericardium (15).

This mathematical modelling leads us to conclude that the additional volume from massive resuscitation in a consistently euvoluemic patient will not precipitate heart failure. Other factors must be considered as plausible aetiologies for a patient's decompensated heart in this clinical setting.

Lauren Correa[1] [iD], Joshua Sappenfield[2] [iD],
Christopher Giordano[2] [iD]
[1]Department of Anaesthesiology, University of Michigan, Michigan, USA
[2]Department of Anaesthesiology, University of Florida College of Medicine, Florida, USA

References

1. Shiels HA, White E. The Frank-Starling mechanism in vertebrate cardiac myocytes. J Exp Biol 2008; 211: 2005-13. [CrossRef]
2. Ghignone M, Girling L, Prewitt RM. Volume expansion versus norepinephrine in treatment of a low cardiac output complicating an acute increase in right ventricular afterload in dogs. Anesthesiology 1984; 60: 132-5. [CrossRef]

3. Feneley MP, Elbeery JR, Gaynor JW, Gall SA, Davis JW, Rankin JS. Ellipsoidal shell subtraction model of right ventricular volume. Comparison with regional free wall dimensions as indexes of right ventricular function. Circ Res 1990; 67: 1427-36. [CrossRef]

4. Rudski LG, Lai WW, Afilalo J, Hua L, Handschumacher MD, Chandrasekaran K, et al. Guidelines for the echocardiographic assessment of the right heart in adults: A report from the American Society of Echocardiography endorsed by the European Association of Echocardiography, a registered branch of the European Society of Cardiology, and the Canadian Society of Echocardiography. J Am Soc Echocardiogr 2010; 23: 685-713. [CrossRef]

5. Armstrong WF, Ryan T, Feigenbaum H. Feigenbaum's Echocardiography. Philadelphia, PA: Lippincott Williams & Wilkins, 2010: 123.

6. Sonnenblick EH, Spiro D, Spotnitz HM. The ultrastructural basis of Starling's law of the heart. The role of the sarcomere in determining ventricular size and stroke volume. Am Heart J 1964; 68: 336-46. [CrossRef]

7. Warren JV, Brannon ES. Effect of increasing the blood volume and right atrial pressure on the circulation of normal subjects by intravenous infusions. Am J Med 1948; 4: 193-200. [CrossRef]

8. Gan C, Lankhaar JW, Marcus JT, Westerhof N, Marques KM, Bronzwaer JG, et al. Impaired left ventricular filling due to right-to-left ventricular interaction in patients with pulmonary arterial hypertension. Am J Physiol Heart Circ Physiol 2006; 290: H1528-33.

9. Smith HM, Farrow SJ, Ackerman JD, Stubbs JR, Sprung J. Cardiac arrests associated with hyperkalemia during red blood cell transfusion: A case series. Anesth Analg 2008; 106: 1062-9. [CrossRef]

10. Lualdi JC, Goldhaber SZ. Right ventricular dysfunction after acute pulmonary embolism: Pathophysiologic factors, detection, and therapeutic implications. Am Heart J 1995; 130: 1276-82. [CrossRef]

11. Lewis ME, Al-khalidi AH, Townend JN, Coote J, Bonser RS. The effects of hypothermia on human left ventricular contractile function during cardiac surgery. J Am Coll Cardiol 2002; 39: 102-8. [CrossRef]

12. Levine SN, Rheams CN. Hypocalcemic heart failure. Am J Med 1985; 78: 1033-5. [CrossRef]

13. Denlinger JK, Nahrwold ML, Gibbs PS, Lecky JH. Hypocalcemia during rapid blood transfusion in anaesthetized man. Br J Anaesth 1976; 48: 995-1000. [CrossRef]

14. Kinsky M, Ribeiro N, Cannesson M, Deyo D, Kramer G, Salter M, et al. Peripheral venous pressure as an indicator of preload responsiveness during volume resuscitation from hemorrhage. Anesth Analg 2016; 123: 114-22. [CrossRef]

15. Hoit BD, Dalton N, Bhargava V, Shabetai R. Pericardial influences on right and left ventricular filling dynamics. Circ Res 1991; 68: 197-208. [CrossRef]

Corresponding Author/Sorumlu Yazar: Joshua Sappenfield

E-mail: jsappenfield@anest.ufl.edu

Appendix 1. Calculations for the Ellipsoid Shell Subtraction Model

Please refer to Figure 2 for the diagram of the model showing all the dimensions.

Dimensions

Diameter 'a': LV height (major axis)
Diameter 'b': LV anteroposterior (minor axis)
Diameter 'c': LV septal-free wall diameter
Diameter 'd': RV septal-free wall diameter
FWV=free wall volume

Values

'a': RV height=2/3 LV height
    LV height=3/2 RV height
    LV height=3/2(7.1 cm)
    LV height=**10.65 cm**
'b': LV diastolic diameter=**5.05 cm**
'd': RV septal-free wall diameter=**2.8 cm**

Equation for the RV Volume

$RVV_{in}=\frac{\pi}{6}ab(c+d)-\pi abc-FWV$
$RVV_{in}=\frac{\pi}{6}abd-FWV$
$\mathbf{RVV_{in}=V=\frac{\pi}{6}abd}$

Proportions

$a=\frac{10.65}{2.8}d$ $b=\frac{5.05}{2.8}d$

Proof of Proportions

$V=\frac{\pi}{6}abd$
$V=\frac{\pi}{6}(10.65)(5.05)(2.8)$
$V=78.849$

$78.849=\frac{\pi}{6}abd$
$\frac{6}{\pi}(78.849)=abd$
$150.591=abd$
$150.591=(\frac{10.65}{2.8}d)(\frac{5.05}{2.8}d)d$
$150.591=6.861d^3$
$21.948=d^3$
$d=2.8$

Derivation of equation for volume and diameter

$V=\frac{\pi}{6}abd$
$\frac{6}{\pi}V=(\frac{10.65}{2.8}d)(\frac{5.05}{2.8}d)d$
$\frac{6}{\pi}V=(3.804\ d)(1.804\ d)d$
$\frac{6}{\pi}V=6.861d^3$
$\frac{6}{(6.681)\pi}V=d^3$
$0.278V=d^3$
$\mathbf{V=3.597d^3}$

$d^3=\frac{V}{3.597}$
$\mathbf{d=\sqrt[3]{0.278\ V}}$

Appendix 2. Ellipsoid-Percent Stretch after Infusion

Heart Rate (BPM)	Cardiac Output (mL min⁻¹)	End Diastolic Volume (EDV) (mL)	Infusion Rate (mL min⁻¹)	Additional Volume per Beat (mL)	EDV during Infusion (mL)	% Stretch
60	2000	55.6	500	8.3	63.9	4.8
			750	12.5	68.1	7.0
			1000	16.7	72.3	9.1
			1500	25.0	80.6	13.2
60	4000	111.1	500	8.3	119.4	2.4
			750	12.5	123.6	3.6
			1000	16.7	127.8	4.8
			1500	25.0	136.1	7.0
60	6000	166.7	500	8.3	175.0	1.6
			750	12.5	179.2	2.4
			1000	16.7	183.4	3.2
			1500	25.0	191.7	4.8
60	8000	222.2	500	8.3	230.5	1.2
			750	12.5	234.7	1.8
			1000	16.7	238.9	2.4
			1500	25.0	247.2	3.6
90	2000	37.0	500	5.6	42.6	4.8
			750	8.3	45.3	7.0
			1000	11.1	48.1	9.1
			1500	16.7	53.7	13.2
90	4000	74.1	500	5.6	79.7	2.4
			750	8.3	82.4	3.6
			1000	11.1	85.2	4.8
			1500	16.7	90.8	7.0
90	6000	111.1	500	5.6	116.7	1.6
			750	8.3	119.4	2.4
			1000	11.1	122.2	3.2
			1500	16.7	127.8	4.8
90	8000	148.1	500	5.6	153.7	1.2
			750	8.3	156.4	1.8
			1000	11.1	159.2	2.4
			1500	16.7	164.8	3.6
120	2000	27.8	500	4.2	32.0	4.8
			750	6.3	34.1	7.0
			1000	8.3	36.1	9.1
			1500	12.5	40.3	13.2
120	4000	55.6	500	4.2	59.8	2.4
			750	6.3	61.9	3.6
			1000	8.3	63.9	4.8
			1500	12.5	68.1	7.0
120	6000	83.3	500	4.2	87.5	1.6
			750	6.3	89.6	2.4
			1000	8.3	91.6	3.2
			1500	12.5	95.8	4.8
120	8000	111.1	500	4.2	115.3	1.2
			750	6.3	117.4	1.8
			1000	8.3	119.4	2.4
			1500	12.5	123.6	3.6